

# CIAMA: A new multiple access scheme

Jianjian Wu, Qingfeng Zhou, *Member, IEEE*

**Abstract**—This paper studies advanced multi-access techniques to support a high volume of concurrent access demanded in future wireless networks. Sparse code multiple access (SCMA), as a code-domain Non-Orthogonal Multiple Access (NOMA), serves multiple users simultaneously by frequency-domain coding. Blind Interference Alignment on the other hand applies time-domain coding to accommodate multiple users. Unlike beamforming, both of them need no CSIT, which saves the control cost of channel information feedback and highly simplifies the implementation of multiple access. To achieve even higher multiplexing gain and diversity order, we propose a new multiple access framework, which makes use of both time and frequency coding by combining SCMA and BIA, and is named as SparseCode-and-BIA-based multiple access (CIAMA). Then we analyze two decoding schemes, the two-stage decoding scheme consisting of zero-forcing and Message Passing Algorithm (MPA), and the Joint Message Passing Algorithm (JMPA) enhanced by constructing a virtual factor graph. Simulation results indicate that although the two-stage decoding performance is inferior to both BIA and SCMA, it has low decoding complexity. On the other hand, the JMPA decoding scheme achieves the same diversity gain as STBC-based SCMA while gaining even higher multiplexing gain, which makes the CIAMA with JMPA decoding scheme an attractive MA scheme in future wireless communication networks.

**Index Terms**—MISO interference, Blind interference alignment, reconfigurable antenna.

## I. INTRODUCTION

Wireless networks constantly face the challenge of multiple access. To meet the growing need for communications, fifth-generation (5G) wireless networks implement various technologies such as massive Multiple Input Multiple Output (MIMO) and millimeter microwave (mm-Wave) [1]. The increasing deployment of micro-cells to enhance data transfer rates and densify network connections further complicates multi-user access [2], [3]. Researchers increasingly show interest in 6G evolution, which is projected to have approximately 100 times more connection density than 5G, causing significant multi-user interference [4].

Orthogonal techniques such as Frequency Division Multiple Access (FDMA), Time Division Multiple Access (TDMA), Code Division Multiple Access (CDMA), and Orthogonal Frequency Division Multiple Access (OFDMA) have been used to manage multi-user interference in earlier wireless communication systems [5]. These techniques divide wireless resource in an "orthogonal" manner, enabling exclusive access to a fraction of wireless resource by individual user, thereby avoiding interference [6]. However, such an approach cannot handle the demand for massive access due to limited resource.

To attain higher spectral efficiency, researchers are studying non-orthogonal techniques such as Interference alignment (IA) [7] and Non-Orthogonal Multiple Access (NOMA) [8]. IA aligns multiple interference signal vectors into a small subspace and reserves the remaining subspace for transmitting the intended signal [9]. Given its potential to reach the capacity of interference channels, researchers have incorporated IA into several communication systems, including cognitive radio networks [10], cellular networks [11], heterogeneous networks [12], and Device-to-Device (D2D) networks [13]. NOMA utilizes superposition coding to allow multiple users to transmit signals on the same resource block, for instance, time and frequency. Two types of NOMA have been proposed, Power-Domain NOMA (PD-NOMA) and Code-Domain NOMA (CD-NOMA). Signals at the receivers are decoded by using Successive Interference Cancellation (SIC) or Message Passing Algorithm (MPA). NOMA can combine with other existing technologies such as massive MIMO [15], mm-Wave [16], etc.. NOMA is gaining attention in 5G and is expected to be a key technique in future communication networks [14].

Throughout the development of IA, a primary limitation is the requirement for channel state information at the transmitter (CSIT) [17]. In order to eliminate the relying on CSIT, researchers have introduced blind IA (BIA) [18]. BIA works under predefined channel patterns and can be fulfilled by two methods: channel-based BIA (CB-BIA) and reconfigurable-antenna-based BIA (RA-BIA). BIA carries out transmission using specially designed channel patterns, often referred to as "supersymbols," over several symbol extensions. The overhead cost associated with mode-switching is considered in [19], which proposed methods to achieve the minimum overall number of mode-switching instances among various users. Furthermore, a balanced-switching-oriented BIA plan is formulated, which maintains a similar total number of mode-switching instances as that of current schemes [20].

PD-NOMA schemes also require information on channel information [21]. With CSIT available, some researchers have introduced IA into PD-NOMA systems [22]. Hybrid schemes are typically more practical compared to IA-only schemes and exhibit superior performance relative to NOMA-only systems. For instance, IA is employed to manage inter-cell and inter-cluster interferences in multi-cell NOMA systems [23]. In light of the additional overhead involved with CSIT, some scholars have introduced blind IA (BIA) into PD-NOMA systems, as discussed in [24]. According to the suggested scheme, BIA effectively mitigates interferences between clusters without the need for moment-by-moment access to CSIT, and offers better results compared to conventional MISO-NOMA techniques. While the proposed scheme is independent of instantaneous CSIT, its integration into multi-carrier systems is not straight-

Corresponding author: Qingfeng Zhou (e-mail: enqfzhou@ieee.org). J. Wu and Q.F. Zhou are with the School of Electric Engineering and Intelligentization, Dongguan University of Technology, Dongguan 523808, China. J. Wu is also with the School of Computer science and Information engineering, Hefei University of Technology, Hefei 230601, China.

forward [24].

PD-NOMA techniques typically demand CSIT for efficient power allocation, which limits their feasibility in systems with limited or no access to CSIT. To fit such systems, the sparse code multiple access (SCMA) technique is a feasible alternative in code-domain NOMA, as highlighted in [25]. In multi-carrier systems, both low-density multi-dimensional codebooks and message passing algorithms (MPA) are employed, which enable multi-subcarrier diversity gain and unique "shaping gain" to be advantageous for SCMA, as explained in [26]. The optimal codebook design for SCMA is still being debated due to its complexity. The authors in [28] suggest a low-complexity construction method as well as a systematic construction process for the near-optimal codebook design. The low-complexity decoding architecture of SCMA is also a hot topic. Scholars have attempted to simplify the task by adapting MPA to the logarithmic domain, proposing techniques such as Log-MPA and MAX-Log-MPA, which reduce the number of exponential operations required in the original MPA. While low-complexity MPA techniques have been proposed, the design of decoders for MIMO-SCMA systems remains challenging because the decoding complexity increases exponentially with the number of users [30]. Additionally, scholars have incorporated space-time block coding (STBC) into MIMO-SCMA systems, which offers a higher diversity order [29]. Although the STBC-SCMA scheme offers additional diversity over multiple antennas, its multiplexing gain is limited. Another limitation of existing SCMA schemes is the potential for privacy breaches in multi-user systems. In such systems, each receiver uses MPA to decode not only the desired signal, but also interference signals, as multi-user signals are simply superimposed over the code domain, which can allow for unauthorized access to data from other users.

BIA and SCMA have the potential to adapt to systems with partial or no channel state information, making these two techniques more robust than other CSIT-based methods. However, BIA and SCMA are implemented in different domains, no studies have yet examined their combination. This paper fills the gap, and proposes a method to combine SCMA and BIA while achieving even higher diversity order and multiplexing gain. In our proposed scheme, transmitted signals are first mapped by SCMA codebooks, and the resulting codewords are then encoded by the BIA principle. At the receiver, two decoding schemes are employed. The first is a two-stage scheme that employs zero-forcing and then a message passing algorithm (MPA). The second scheme is the joint message passing algorithm (JMPA), and its key is to construct a virtual factor graph. The complexity of the two-stage decoder is linear with the number of users, but its performance is limited. The JMPA decoder achieves the same diversity order as the space-time block coded SCMA (STBC-SCMA) scheme, with the same cost of complexity. Our proposed scheme is suitable for systems lacking instantaneous channel state information and achieves a higher multiplexing gain while maintaining the same diversity gain as STBC-SCMA. Moreover, our scheme performs better on data privacy existing MIMO-SCMA schemes, since we employ BIA to manage multi-user interference.

TABLE I  
SUPERSYMBOL OF BIA

	slot-1	slot-2	slot-3	slot-4	slot-5	slot-6	slot-7
$R_1$	$\mathbf{h}_1^j(1)$	$\mathbf{h}_1^j(2)$	$\mathbf{h}_1^j(1)$	$\mathbf{h}_1^j(1)$	$\mathbf{h}_1^j(1)$	$\mathbf{h}_1^j(1)$	$\mathbf{h}_1^j(1)$
$R_2$	$\mathbf{h}_2^j(1)$	$\mathbf{h}_2^j(1)$	$\mathbf{h}_2^j(2)$	$\mathbf{h}_2^j(1)$	$\mathbf{h}_2^j(1)$	$\mathbf{h}_2^j(1)$	$\mathbf{h}_2^j(1)$
$R_3$	$\mathbf{h}_3^j(1)$	$\mathbf{h}_3^j(1)$	$\mathbf{h}_3^j(1)$	$\mathbf{h}_3^j(2)$	$\mathbf{h}_3^j(1)$	$\mathbf{h}_3^j(1)$	$\mathbf{h}_3^j(1)$
$R_4$	$\mathbf{h}_4^j(1)$	$\mathbf{h}_4^j(1)$	$\mathbf{h}_4^j(1)$	$\mathbf{h}_4^j(1)$	$\mathbf{h}_4^j(2)$	$\mathbf{h}_4^j(1)$	$\mathbf{h}_4^j(1)$
$R_5$	$\mathbf{h}_5^j(1)$	$\mathbf{h}_5^j(1)$	$\mathbf{h}_5^j(1)$	$\mathbf{h}_5^j(1)$	$\mathbf{h}_5^j(1)$	$\mathbf{h}_5^j(2)$	$\mathbf{h}_5^j(1)$
$R_6$	$\mathbf{h}_6^j(1)$	$\mathbf{h}_6^j(1)$	$\mathbf{h}_6^j(1)$	$\mathbf{h}_6^j(1)$	$\mathbf{h}_6^j(1)$	$\mathbf{h}_6^j(1)$	$\mathbf{h}_6^j(2)$

## II. SYSTEM MODEL

Consider a  $K$ -user  $N_t \times 1$  MISO broadcast channel with  $J$  tones, e.g., OFDM subcarriers, available for transmission. It is assumed that  $K = 6$ ,  $J = 4$ , the base station has  $N_t = 2$  traditional antennas, and each receiver/user equips a reconfigurable antenna (RA). The same as the general assumption in previous RA-based BIA, we suppose a RA can artificially switch its operation mode, thus change its channel state. The RA can switch  $N_t = 2$  modes at each user. In this paper, we suppose no CSI at the BS and full CSI at all receivers.

The composite channel model applied considers both quasi-static Rayleigh fading and large-scale path loss. Denote  $\mathbf{h}_k^j(m) = \frac{\mathbf{g}_k^j(m)}{\sqrt{D(d_k)}}$  as the channel matrix from the base station to the Rx- $k$  while its RA operating at the  $m$ -th mode on the  $j$ -th tones, where  $\mathbf{h}_k^j, \mathbf{g}_k^j(m) \in \mathbb{C}^{1 \times N_t}$  and  $\mathbf{g}_k^j(m)$  denotes an Rayleigh fading channel matrix.  $d_k$  is the distance between the  $k$ -th user and the BS. The path loss function is denoted as

$$D(d_k) = \begin{cases} d_k^\alpha, & \text{if } d_k > r_0 \\ r_0^\alpha, & \text{otherwise} \end{cases},$$

where  $\alpha$  denotes the path loss exponent and the parameter  $r_0$  avoids a singularity when the distance is small. Without loss of generality, we choose  $\alpha = 3$ . Assume all users has the same distance to the BS. Note that we assume the channel state over different antennas and tones are independent and the coherence time over all channels is long enough, e.g., each channel state keeps unchanged over a whole transmission progress. We further denotes  $E_s$  as the total transmit power at the BS.

### A. Blind Interference alignment

In this section, the BIA scheme based on reconfigurable antennas (RA) is utilized in the system [18]. It is assumed that reconfigurable antennas can switch their operation mode and hence artificially change the channel state. Take advantage of this property, we utilize RA to artificially reconstruct the channel patterns, hence satisfying feasible conditions for BIA. The result channel patterns are also called "supersymbols". To decode intended signals, a decoding beamforming vector is designed for each user, respectively. As an example, the

$R_1$	$\mathbf{V}_1 = [\mathbf{I} \mathbf{1} \mathbf{0} \mathbf{0} \mathbf{0} \mathbf{0}]^T$
$R_2$	$\mathbf{V}_2 = [\mathbf{I} \mathbf{0} \mathbf{1} \mathbf{0} \mathbf{0} \mathbf{0}]^T$
$R_3$	$\mathbf{V}_3 = [\mathbf{I} \mathbf{0} \mathbf{0} \mathbf{1} \mathbf{0} \mathbf{0}]^T$
$R_4$	$\mathbf{V}_4 = [\mathbf{I} \mathbf{0} \mathbf{0} \mathbf{0} \mathbf{1} \mathbf{0}]^T$
$R_5$	$\mathbf{V}_5 = [\mathbf{I} \mathbf{0} \mathbf{0} \mathbf{0} \mathbf{0} \mathbf{1}]^T$
$R_6$	$\mathbf{V}_6 = [\mathbf{I} \mathbf{1} \mathbf{0} \mathbf{0} \mathbf{0} \mathbf{0}]^T$

Fig. 1. Beamforming vectors of BIA

supersymbol and transmit beamforming vectors  $\mathbf{V}_k$  on the  $j$ -th tone can be shown as Table.I and Fig.1, respectively. Note that we have  $J$  subcarriers in the system, here we consider independent BIA design at each subcarrier.

Without loss of generality, Consider the  $j$ -th tones at the first user, the received signal can be expressed as

$$\begin{aligned} \mathbf{Y}_1^j &= \mathcal{H}_k^j \left( \mathbf{V}_1 \mathbf{u}_1^j + \mathbf{V}_2 \mathbf{u}_2^j + \mathbf{V}_3 \mathbf{u}_3^j + \mathbf{V}_4 \mathbf{u}_4^j + \mathbf{V}_5 \mathbf{u}_5^j + \mathbf{V}_6 \mathbf{u}_6^j \right) + \mathbf{Z}_1^j \\ &= \begin{bmatrix} \mathbf{h}_1^j(1) \\ \mathbf{h}_1^j(2) \\ \mathbf{0} \\ \mathbf{0} \\ \mathbf{0} \\ \mathbf{0} \end{bmatrix} \mathbf{u}_1^j + \begin{bmatrix} \mathbf{h}_1^j(1) \\ \mathbf{0} \\ \mathbf{h}_1^j(1) \\ \mathbf{0} \\ \mathbf{0} \\ \mathbf{0} \end{bmatrix} \mathbf{u}_2^j + \begin{bmatrix} \mathbf{h}_1^j(1) \\ \mathbf{0} \\ \mathbf{0} \\ \mathbf{h}_1^j(1) \\ \mathbf{0} \\ \mathbf{0} \end{bmatrix} \mathbf{u}_3^j \\ &+ \begin{bmatrix} \mathbf{h}_1^j(1) \\ \mathbf{0} \\ \mathbf{0} \\ \mathbf{0} \\ \mathbf{h}_1^j(1) \\ \mathbf{0} \end{bmatrix} \mathbf{u}_4^j + \begin{bmatrix} \mathbf{h}_1^j(1) \\ \mathbf{0} \\ \mathbf{0} \\ \mathbf{0} \\ \mathbf{0} \\ \mathbf{h}_1^j(1) \end{bmatrix} \mathbf{u}_5^j + \begin{bmatrix} \mathbf{h}_1^j(1) \\ \mathbf{0} \\ \mathbf{0} \\ \mathbf{0} \\ \mathbf{0} \\ \mathbf{h}_1^j(1) \end{bmatrix} \mathbf{u}_6^j \\ &+ \mathbf{Z}_1^j \end{aligned} \quad (1)$$

where

$$\mathcal{H}_k^j = \begin{bmatrix} \mathbf{h}_1^j(1) & \mathbf{0} & \dots & \dots & \dots & \dots & \mathbf{0} \\ \mathbf{0} & \mathbf{h}_1^j(2) & & & & & \vdots \\ \vdots & & \mathbf{h}_1^j(1) & & & & \vdots \\ \vdots & & & \mathbf{h}_1^j(1) & & & \vdots \\ \vdots & & & & \mathbf{h}_1^j(1) & & \vdots \\ \vdots & & & & & \mathbf{h}_1^j(1) & \mathbf{0} \\ \mathbf{0} & \dots & \dots & \dots & \mathbf{0} & \dots & \mathbf{h}_1^j(1) \end{bmatrix} \quad (2)$$

is the corresponding channel matrix according to the supersymbol and  $\mathbf{u}_k^j \in \mathbb{C}^{N_t \times 1}$  is the transmit complex vector for the  $k$ -th user at the  $j$ -th tone. For decoding its desired signals, a post-processing matrix  $\mathbf{P}_1 = \begin{bmatrix} \frac{1}{\sqrt{6}} & 0 & -\frac{1}{\sqrt{6}} & -\frac{1}{\sqrt{6}} & -\frac{1}{\sqrt{6}} & -\frac{1}{\sqrt{6}} & -\frac{1}{\sqrt{6}} \\ 0 & 1 & 0 & 0 & 0 & 0 & 0 \end{bmatrix}$  is utilized, hence we have

$$\mathbf{P}_1 \mathbf{Y}_1^j = \begin{bmatrix} \frac{1}{\sqrt{6}} \mathbf{h}_1^j(1) \\ \mathbf{h}_1^j(2) \end{bmatrix} \mathbf{u}_1^j + \tilde{\mathbf{Z}}_1^j \quad (3)$$

TABLE II  
ALAMOUTI CODE

	slot 1	slot 2
Antenna A	$x^{j(1)}$	$-x^{j(2)*}$
Antenna B	$x^{j(2)}$	$x^{j(1)*}$

Consequently an equivalent  $2 \times 2$  MIMO channel is achieved and traditional MIMO detectors can be readily introduced, e.g., zero-forcing decoder and MMSE decoder.

### B. Sparse code multiple access

In this section, traditional SCMA scheme is introduced. Fig 2 is the SCMA encoding diagram at the  $n_t$ -th antenna. In this model,  $\mathbf{b}_k^{(n_t)}$  denotes the binary input for the  $k$ -th user at the  $n_t$ -th antenna. After the SCMA encoder,  $\mathbf{b}_k^{(n_t)}$  is mapped to a complex codeword  $\mathbf{s}_k^{(n_t)} = [s_k^{1(n_t)}, \dots, s_k^{J(n_t)}]^T$  for user- $k$  from the  $n_t$ -th antenna over  $J$  subcarriers. Denotes an indicator matrix as  $F = [f_1 \dots f_K]$ , where '1' in  $f_k$  denotes the positions of non-zero elements in  $\mathbf{s}_k^{(n_t)}$ . Suppose that  $K = 6$  and  $J = 4$ , a widely used indicator matrix is considered

$$F = \begin{bmatrix} 1 & 1 & 1 & 0 & 0 & 0 \\ 1 & 0 & 0 & 1 & 1 & 0 \\ 0 & 1 & 0 & 1 & 0 & 1 \\ 0 & 0 & 1 & 0 & 1 & 1 \end{bmatrix} \quad (4)$$

Note that the indicator matrix design influence the decoding complexity and accuracy much, we used here provides a moderate performance and computation consumption. Here each user only transmit signals on two different tones, respectively.

The received signal of user- $k$  can be written as

$$\mathbf{y}_k = \sum_{n_t=1}^{N_t} \text{diag}(\mathbf{h}_k^{(n_t)}) \mathbf{x}^{(n_t)} = \sum_{n_t=1}^{N_t} \text{diag}(\mathbf{h}_k^{(n_t)}) \sum_{i=1}^K \mathbf{s}_i^{(n_t)} + \mathbf{n}_k \quad (5)$$

Where  $\mathbf{x}^{(n_t)} = [x^{1(n_t)}, \dots, x^{J(n_t)}]^T = \sum_{k=1}^K \mathbf{s}_k^{(n_t)}$  denotes the superposed signals for six users over four tones, and  $\mathbf{h}_k^{(n_t)} \in \mathbb{C}^{J \times 1}$  denotes the channel coefficient vector of the  $n_t$ -th antenna of the user- $k$  over all subcarriers.

The multi-antenna SCMA does not utilize any multi antenna gain, e.g, diversity gain and multiplexing gain. In this subsection, traditional MIMO technique, space-time block code, is introduced into the multi antenna SCMA system. Table.II shows the conventional STBC, Alamouti code, in a two user  $2 \times 1$  BC at the  $j$ -th tone<sup>1</sup>. By utilizing the Alamouti code, two different symbols are transmitted over two antennas through two slots. Note that diversity gain is realized.

Differ from the abovementioned Multi-antenna SCMA, the STBC-SCMA transmit different symbols at two antennas, i.e.,  $s_i^{(1)} \neq s_i^{(2)}$  and  $x^{j(1)} \neq x^{j(2)}$ . Thus for the  $j$ -th subcarrier,  $x^{j(1)}$  and  $x^{j(2)}$  are transmit through the Alamouti code over two slots.

<sup>1</sup>Note that in this paper we use  $x^*$  to denotes the conjugate of a complex number  $x$ .

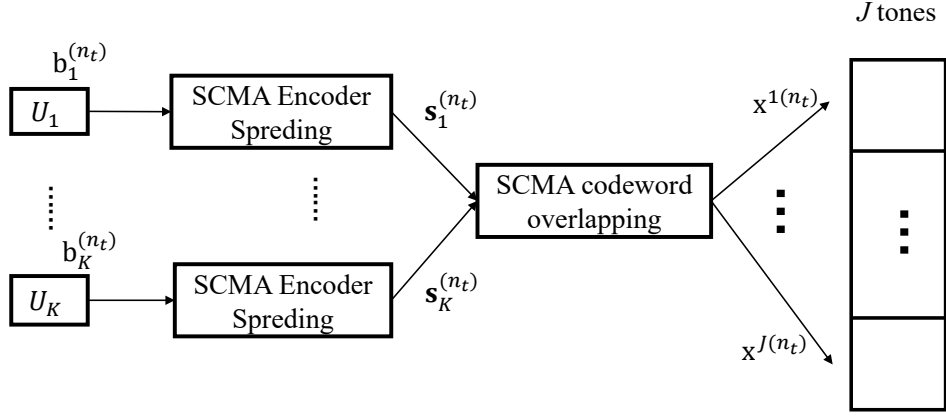


Fig. 2. Encoding block diagram of SCMA.

According the Alamouti design, the received signals of the  $k$ -th user at the  $j$ -th subcarrier are

$$\begin{aligned} \begin{bmatrix} y_k^j(1) \\ y_k^j(2) \end{bmatrix} &= \begin{bmatrix} h_k^{j(1)} & h_k^{j(2)} \\ h_k^{j(2)*} & -h_k^{j(1)*} \end{bmatrix} \begin{bmatrix} x_k^j(1) \\ x_k^j(2) \end{bmatrix} + \begin{bmatrix} z_k^{j(1)} \\ z_k^{j(2)*} \end{bmatrix} \\ &= \begin{bmatrix} h_k^{j(1)} & h_k^{j(2)} \\ h_k^{j(2)*} & -h_k^{j(1)*} \end{bmatrix} \begin{bmatrix} \sum_{i=1}^6 s_i^{j(1)} \\ \sum_{i=1}^6 s_i^{j(2)} \end{bmatrix} + \begin{bmatrix} z_k^{j(1)} \\ z_k^{j(2)*} \end{bmatrix} \end{aligned} \quad (6)$$

Where  $h_k^{j(n_t)}$  denotes the CSI from the  $n_t$ -th antenna of the BS to the  $k$ -th user at the  $j$ -th subcarrier.

Note that for STBC-SCMA decoder, there are two optional principles: two-stage decoder and joint MPA. The two-stage decoder is to perform a traditional linear STBC decoder, hence performing MPA. The joint MPA is to construct a virtual factor graph and performs MPA decoding according to received signals directly. Note that the decoder designs for our proposed scheme are similar to STBC-SCMA decoder, thus we elaborate the details of the decoder in the section.III.

### III. SPARSECODE-AND-BIA-BASED MA

#### A. Encoding design

Fig.3 shows the diagram of the encoding design when  $K = 6$ ,  $J = 4$  and  $N_t = 2$ . The encoding process can be presented as two steps: SCMA encoding and BIA encoding.

1) *Step 1 - SCMA encoding*: For each  $U_k$ , assume transmitting data  $\mathbf{u}_k^{(n_t)}$  at the  $n_t$ -th transmit antenna, where  $\mathbf{u}_k^{(n_t)}$  is a  $L$ -dimension<sup>2</sup> vector and its  $i$ -th element  $\mathbf{u}_k^{(n_t)}(i)$  is a one-bit binary variable. Like traditional MIMO-SCMA systems, transmitting data over all antennas can be allocated to multiple users. For simplicity, in this paper we assume  $U_k$  for a single user in Fig.3. The SCMA encoders can be defined as  $\mathbf{f} : \mathbb{B} \rightarrow \mathcal{S}$ ,  $\mathbf{s}_{ki}^{(n_t)} = \mathbf{f}(\mathbf{u}_k^{(n_t)}(i))$ , where  $\mathcal{S} \in \mathbb{C}^J$  and  $\|\mathcal{S}\| = 2$ . The SCMA codeword  $\mathbf{s}_{ki}^{(n_t)} \in \mathbb{C}^{J \times 1}$  is a sparse vector and selected from the codebook  $\mathbf{C}_{ki}^{(n_t)}$  of layer- $i$ . In this paper we can use the same codebook  $\mathbf{C}_{ki}^{(n_t)}$  for different  $k$  and  $(n_t)$ . The reasons are: 1) Since user interference is fully eliminated by BIA, different users can share same codebooks to simplify the

system design. 2) The channel uncorrelation assumption allows data streams for different antennas share the same codebook. Thus for the sake of simplicity, we use  $\mathbf{C}_i$  to denote the  $i$ -th layer codebook in the rest of the paper.

After the SCMA encoding, each element in  $\mathbf{u}_k^{(n_t)}(i)$  is mapped into a codeword and superposed over  $J$  tones, producing the transmitting symbol vector  $\mathbf{S}_k^{(n_t)} = \sum_{i=1}^L \mathbf{s}_{ki}^{(n_t)} = [\mathbf{S}_k^{1(n_t)} \dots \mathbf{S}_k^{J(n_t)}]^T$ . Since  $N_t = 2$ , thus  $\mathbf{S}_k^{(1)}$  and  $\mathbf{S}_k^{(2)}$  are reconstructed, and for each tone we have a reconstructed symbol vector  $\mathbf{x}_k^j = [\mathbf{S}_k^{j(1)} \mathbf{S}_k^{j(2)}]^T$ .

2) *Step 2 - BIA encoding*: BIA encoding is applied at each tone by employing symbol extension in time domain. Focusing at the  $j$ -th tone, the transmit vector after reconfigurable-antenna-based BIA can be derived as

$$\mathbf{x}^j = \begin{bmatrix} \mathbf{x}^j(1) \\ \mathbf{x}^j(2) \\ \mathbf{x}^j(3) \\ \mathbf{x}^j(4) \\ \mathbf{x}^j(5) \\ \mathbf{x}^j(6) \\ \mathbf{x}^j(7) \end{bmatrix} = \begin{bmatrix} \mathbf{x}_1^j + \mathbf{x}_2^j + \mathbf{x}_3^j + \mathbf{x}_4^j + \mathbf{x}_5^j + \mathbf{x}_6^j \\ \mathbf{x}_1^j \\ \mathbf{x}_2^j \\ \mathbf{x}_3^j \\ \mathbf{x}_4^j \\ \mathbf{x}_5^j \\ \mathbf{x}_6^j \end{bmatrix} \quad (7)$$

where  $\mathbf{x}_k^j(t) \in \mathbb{C}^{N_r \times 1}$  denotes the transmit vector from the BS in the  $k$ -th tone at the  $t$ -th slot.

After the CIAMA encoding, the receive signals at the first user can be formulated as

$$\mathbf{Y}_1 = \left[ (\mathbf{y}_1^1)^T \dots (\mathbf{y}_1^J)^T \right]^T \quad (8)$$

where the receive signals at on the  $j$ -th tone over 7 slots are

$$\begin{aligned} \mathbf{y}_1^j &= [y_1^j(1) \ y_1^j(2) \ \dots \ y_1^j(7)]^T \\ &= \begin{bmatrix} \mathbf{h}_1^j(1) & \mathbf{0} & \dots & \mathbf{0} \\ \mathbf{0} & \mathbf{h}_1^j(2) & \dots & \mathbf{0} \\ \vdots & \vdots & \ddots & \mathbf{0} \\ \mathbf{0} & \mathbf{0} & \mathbf{0} & \mathbf{h}_1^j(1) \end{bmatrix} \begin{bmatrix} \mathbf{x}^j(1) \\ \vdots \\ \mathbf{x}^j(7) \end{bmatrix} + \mathbf{Z}_1^{(j)} \end{aligned} \quad (9)$$

Here  $\mathbf{Z}_1^{(j)} = [z_1^j(1) \ \dots \ z_1^j(7)]^T$  is the additive gaussian noise vector over 7 slots.

<sup>2</sup>Note: The value of  $L$  depends on the number of available subcarriers,  $J$ , and the predetermined degree of resource reuse.

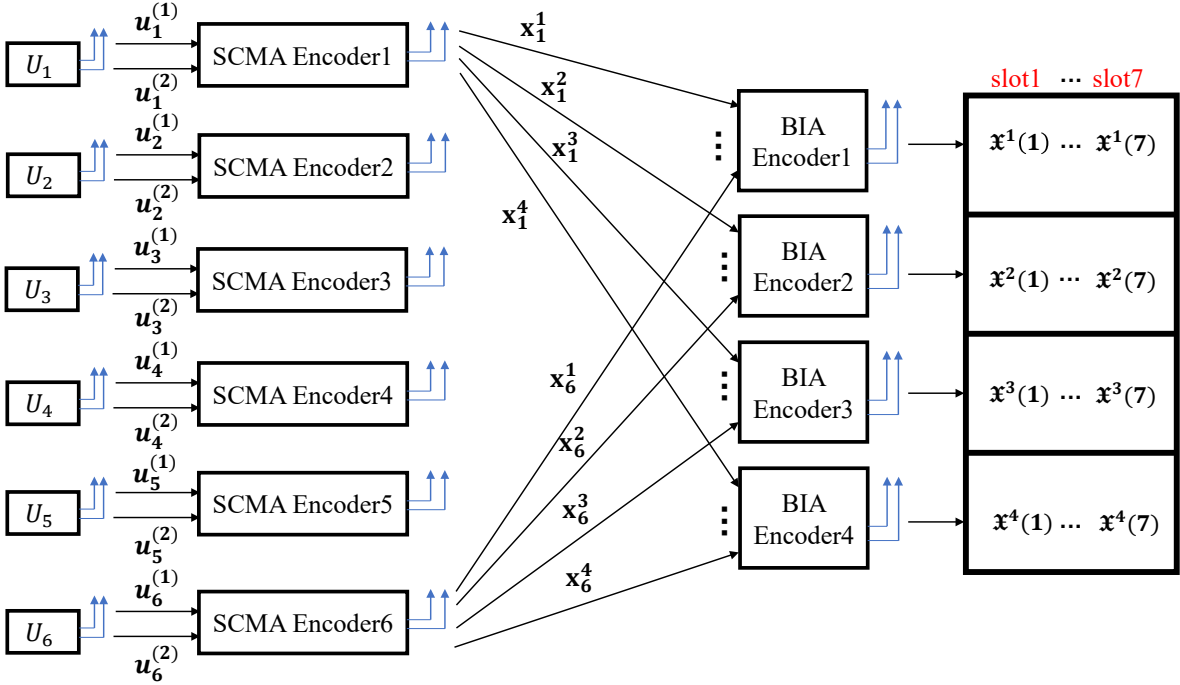


Fig. 3. Encoding diagram of the proposed scheme

### B. Two stage Decoding

In this section, the two-step decoding design is proposed. We firstly employ a traditional MIMO detector (Zero-forcing detector) to separate space data flow, then a traditional log-MPA is applied to decode SCMA signals. By this design, low decoding complexity is achieved but the performance needs to be improved.

Based on the received signal vector, we design our decoding process by firstly applying the BIA decoder and then the MPA decoder. After the BIA decoder, multi-user interference are fully suppressed and the multiple spatial data flow can be untied. Further, each user can apply simple MPA decoder for its own data at each spatial data flow.

1) *BIA decoding*: In this step, we apply the BIA decoding for signals over each tones, respectively. A BIA decoding matrix  $\mathbf{P}_k$  is firstly used for the  $k$ -th user at each tone, e.g.,  $\mathbf{P}_1 = \begin{bmatrix} \frac{1}{\sqrt{6}} & 0 & -\frac{1}{\sqrt{6}} & -\frac{1}{\sqrt{6}} & -\frac{1}{\sqrt{6}} & -\frac{1}{\sqrt{6}} & -\frac{1}{\sqrt{6}} \\ 0 & 1 & 0 & 0 & 0 & 0 & 0 \end{bmatrix}$ . Hence the received signals over four tones can be formulated as

$$\begin{aligned} \hat{\mathbf{Y}}_k &= (\mathbf{I}_4 \otimes \mathbf{P}_k) \mathbf{Y}_k \\ &= \begin{bmatrix} \mathbf{H}_k^1 & \mathbf{0} & \mathbf{0} & \mathbf{0} \\ \mathbf{0} & \mathbf{H}_k^2 & \mathbf{0} & \mathbf{0} \\ \mathbf{0} & \mathbf{0} & \mathbf{H}_k^3 & \mathbf{0} \\ \mathbf{0} & \mathbf{0} & \mathbf{0} & \mathbf{H}_k^4 \end{bmatrix} \begin{bmatrix} \mathbf{x}_k^1 \\ \mathbf{x}_k^2 \\ \mathbf{x}_k^3 \\ \mathbf{x}_k^4 \end{bmatrix} + \begin{bmatrix} \hat{\mathbf{Z}}_k^1 \\ \hat{\mathbf{Z}}_k^2 \\ \hat{\mathbf{Z}}_k^3 \\ \hat{\mathbf{Z}}_k^4 \end{bmatrix} \\ &= \hat{\mathbf{H}}_k \mathbf{X}_k + \hat{\mathbf{Z}}_k \end{aligned} \quad (10)$$

where  $\otimes$  denotes the kronecker product and  $\mathbf{H}_k^j = \begin{bmatrix} \frac{1}{\sqrt{6}} \mathbf{h}_k^j(1) & \mathbf{h}_k^j(2) \end{bmatrix}^T \in \mathbb{C}^{2 \times 2}$  is the corresponding channel matrix for the  $k$ -th user at the  $j$ -th tone. Besides, the cor-

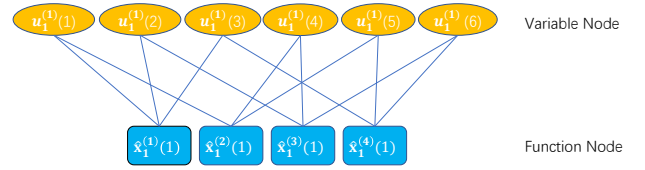


Fig. 4. Factor graph for MPA decoder of one spatial data flow

responding noise vector is

$$\hat{\mathbf{Z}}_k^j = \begin{bmatrix} \frac{1}{\sqrt{6}} z_k^j(1) - \frac{1}{\sqrt{6}} \left( \sum_{t=3}^7 z_k^j(t) \right) \\ z_k^j(2) \end{bmatrix} \quad (11)$$

Since  $\mathbf{H}_k^j$  is full-rank, here we can simply decode each symbol of  $\hat{\mathbf{Y}}_k$  by zero-forcing. Thus we have untied the two spatial data flow and obtain a estimated vector  $\hat{\mathbf{x}}_k^j$ .

2) *MPA decoding*: Since the BIA decoder have untied the two data flow, we can apply traditional MPA decoder at each spatial data flow. Fig.4 shows the MPA indicator graph for the user-1 at one spatial data flow. Note that the MPA here has smaller computation complexity than that in SCMA, because the CSI is not required in our scheme. In this step, we use  $\hat{\mathbf{x}}_k^{(1)1}, \hat{\mathbf{x}}_k^{(2)1}, \hat{\mathbf{x}}_k^{(3)1}, \hat{\mathbf{x}}_k^{(4)1}$  as function nodes, then we can decode  $\mathbf{u}_k^{(N_t)}$  at the  $N_t$ -th space data flow.

### C. Joint MPA decoding

In this section, a joint MPA design is proposed. In the previous section, the ZF+MPA decoding has a poor performance considering BER because the traditional MIMO detector misfits the SCMA decoding. To further improve the performance, we propose a joint MPA design for the proposed

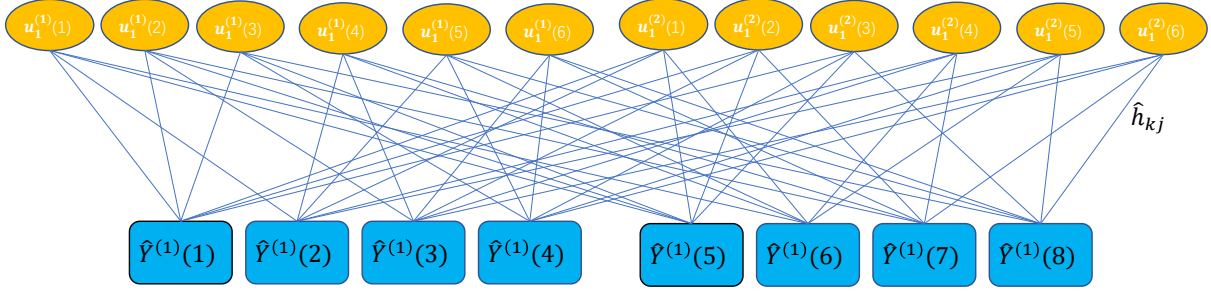


Fig. 5. Factor graph for Joint MPA decoder

scheme, which comes from the traditional joint MPA for MIMO-SCMA.

In this section, the received signal for user-1  $\hat{\mathbf{Y}}_1 \in \mathbb{C}^{(N_r \times J) \times 1}$  are treated as function nodes directly then decode all space data flows simultaneously. Figure.5 shows the virtual indicator graph for the first user. The virtual indicator matrix is

$$\mathbf{F}_v = \begin{bmatrix} \mathbf{F} & \mathbf{F} \\ \mathbf{F} & \mathbf{F} \end{bmatrix} \quad (12)$$

Further, the virtual codebook should be constructed according to the original codebook and CSI. Denotes  $\mathbf{C}_i$  as the origin codebook for  $u_k^{(n_r)}(i)$ . To construct the virtual codebook for the  $k'$ -th VN, we need the corresponding CSI vector  $\hat{\mathbf{h}}_{k'} \in \mathbb{C}^{(N_r \times J) \times M}$ . Here we define

$$\begin{bmatrix} \mathbf{A} & \mathbf{B} \\ \mathbf{C} & \mathbf{D} \end{bmatrix} = \begin{bmatrix} 1 & 0 & 0 & 0 & 0 & 0 & 0 & 0 \\ 0 & 0 & 1 & 0 & 0 & 0 & 0 & 0 \\ 0 & 0 & 0 & 0 & 1 & 0 & 0 & 0 \\ 0 & 0 & 0 & 0 & 0 & 0 & 1 & 0 \\ 0 & 1 & 0 & 0 & 0 & 0 & 0 & 0 \\ 0 & 0 & 0 & 1 & 0 & 0 & 0 & 0 \\ 0 & 0 & 0 & 0 & 0 & 1 & 0 & 0 \\ 0 & 0 & 0 & 0 & 0 & 0 & 0 & 1 \end{bmatrix} \begin{bmatrix} \mathbf{H}_1^1 \\ \mathbf{H}_1^2 \\ \mathbf{H}_1^3 \\ \mathbf{H}_1^4 \end{bmatrix} \quad (13)$$

where  $\mathbf{A}, \mathbf{B}, \mathbf{C}, \mathbf{D} \in \mathbb{C}^{J \times 1}$ . Thus we have

$$[\hat{\mathbf{h}}_1 \quad \dots \quad \hat{\mathbf{h}}_{12}] = \begin{bmatrix} \mathcal{J} \otimes \mathbf{A} & \mathcal{J} \otimes \mathbf{B} \\ \mathcal{J} \otimes \mathbf{C} & \mathcal{J} \otimes \mathbf{D} \end{bmatrix}, \quad (14)$$

where  $\mathcal{J}$  is a all-ones matrix with the size of  $1 \times L$ . Thus the virtual codebook for the  $k'$ -th VN is

$$\hat{\mathbf{C}}_{k'} = \text{diag}(\hat{\mathbf{h}}_{k'}) \begin{bmatrix} \mathbf{C}_g \\ \mathbf{C}_g \end{bmatrix} \quad (15)$$

where

$$g = \begin{cases} k', & k' \leq 6 \\ k' - 6, & 6 < k' \leq 12 \end{cases} \quad (16)$$

With the virtual codebook, we can apply traditional Log-MPA to decode all desired signals.

#### IV. ERROR RATE ANALYSIS

This section gives the error rate analysis for the proposed blind-interference-aligned SCMA. Suppose average power allocation over users and denote  $E_b$  as power allocated for one bit, thus we have

$$\mathbb{E}\{\mathbf{x}_k^j\} = \frac{6 \times 6 \times 2E_b}{6 \times 4 \times 2} = \frac{3E_b}{2}. \quad (17)$$

Note that a '2' in the denominator of Eq.(17), because each symbol is transmitted twice on account of BIA encoder. For analysis, we denote  $\mathbf{x}_k^j = \frac{3E_b}{2} \hat{\mathbf{x}}_k^j$ , where  $\hat{\mathbf{x}}_k^j$  is normalized transmitting symbol for user- $k$  at the  $j$ -th tone. Further we have  $\mathbf{X}_k = \frac{3E_b}{2} \mathbf{X}_k^*$ , where  $\mathbf{X}_k^* = [\hat{\mathbf{x}}_k^1 \quad \hat{\mathbf{x}}_k^2 \quad \hat{\mathbf{x}}_k^3 \quad \hat{\mathbf{x}}_k^4]$ .

According to the received signal, the estimated symbols vector  $\hat{\mathbf{X}}_k^*$  is determined by

$$\hat{\mathbf{X}}_k^* = \arg \min \left\| \hat{\mathbf{Y}}_k - \sqrt{\frac{3E_b}{2N_0}} \hat{\mathbf{H}}_k \mathbf{X}_k^* \right\|_F^2 \quad (18)$$

The conditional pairwise error probability (PEP) defined as the probability of  $\mathbf{X}_k^* \rightarrow \hat{\mathbf{X}}_k^*$  for a fixed channel coefficients can be expressed as

$$\begin{aligned} Pr(\mathbf{X}_k^* \rightarrow \hat{\mathbf{X}}_k^* | \hat{\mathbf{H}}_k) \\ = Q \left( \sqrt{\frac{3E_b}{4N_0}} \left\| \hat{\mathbf{H}}_k (\mathbf{X}_k^* - \hat{\mathbf{X}}_k^*) \right\|_F \right), \end{aligned} \quad (19)$$

where  $Q(x) = \frac{1}{\sqrt{2\pi}} \int_x^\infty e^{-\frac{t^2}{2}} dt$ . To evaluate Eq.(19), we use an upper bound for the Q-function as [31], thus we have

$$\begin{aligned} Pr(\mathbf{X}_k^* \rightarrow \hat{\mathbf{X}}_k^* | \hat{\mathbf{H}}_k) \\ \leq \sum_{n=1}^N a_n \exp \left( -c_n \frac{3E_b}{4N_0} \left\| \hat{\mathbf{H}}_k (\mathbf{X}_k^* - \hat{\mathbf{X}}_k^*) \right\|_F^2 \right), \end{aligned} \quad (20)$$

where  $N, a_n, c_n$  are constants. Note that the upper bound tends to the exact value as  $N$  increases.

Since the fact that

$$\begin{aligned} & \left\| \hat{\mathbf{H}}_k (\mathbf{X}_k^* - \hat{\mathbf{X}}_k^*) \right\|_F^2 \\ & = \text{Tr} \left( \hat{\mathbf{H}}_k (\mathbf{X}_k^* - \hat{\mathbf{X}}_k^*) (\mathbf{X}_k^* - \hat{\mathbf{X}}_k^*)^H \hat{\mathbf{H}}_k^H \right) \\ & = \sum_{l=1}^8 \mathbf{h}_k^l (\mathbf{X}_k^* - \hat{\mathbf{X}}_k^*) (\mathbf{X}_k^* - \hat{\mathbf{X}}_k^*)^H (\mathbf{h}_k^l)^H, \end{aligned} \quad (21)$$

where  $\mathbf{h}_k^l$  is the  $l$ -th row vector of  $\hat{\mathbf{H}}_k$ . Note the matrix  $(\mathbf{X}_k^* - \hat{\mathbf{X}}_k^*) (\mathbf{X}_k^* - \hat{\mathbf{X}}_k^*)^H$  is Hermitian that can be diagonalized by a

unitary transformation, thus we have

$$\begin{aligned} & Pr(\mathbf{X}_k^* \rightarrow \hat{\mathbf{X}}_k^* | \hat{\mathbf{H}}_k) \\ & \leq \sum_{n=1}^N a_n \exp\left(-c_n \frac{3E_b}{4N_0} \sum_{l=1}^8 \mathbf{h}_k^l \mathbf{V}_k \mathbf{\Lambda}_k \mathbf{V}_k^H (\mathbf{h}_k^l)^H\right) \\ & = \sum_{n=1}^N a_n \exp\left(-c_n \frac{3E_b}{4N_0} \sum_{l=1}^8 \sum_{i=1}^8 \lambda_k^i |\mathbf{h}_k^l \mathbf{v}_k^i|^2\right), \end{aligned} \quad (22)$$

where  $\mathbf{\Lambda}_k = \text{diag}(\lambda_k^1, \lambda_k^2, \dots, \lambda_k^8)$ .  $\mathbf{V}_k$  is a unitary matrix and  $\mathbf{v}_k^i = [v_k^{1,i}, v_k^{2,i}, \dots, v_k^{8,i}]$  is the  $i$ -th column of  $\mathbf{V}_k$ .

In this section, we consider rayleigh fading channel, i.e.,  $\mathbf{h}_k^{(j)} \sim \mathcal{CN}(\mathbf{0}, \mathbf{I})$ . Denotes  $|\mathbf{h}_k^l \mathbf{v}_k^i|^2$  as  $\beta_k^{l,i}$ , thus the PDF of the random variable  $\beta_k^{l,i}$  is given by  $f_{\beta_k^{l,i}}(x) = \frac{1}{4b_k^{l,i}} \exp\left(-\frac{x}{4b_k^{l,i}}\right)$ , where  $b_k^{l,i} = \sum_{j=2^{\lfloor \frac{l}{2} \rfloor - 1}}^{2^{\lfloor \frac{l}{2} \rfloor}} T_l |v_k^{j,i}|^2$ , where

$$T_l = \begin{cases} \frac{1}{6}, & l \text{ is odd} \\ 1, & l \text{ is even} \end{cases} \quad (23)$$

Note that  $T_l$  comes from the fact that  $\mathbf{H}_k^{(j)} = \left[ \frac{1}{\sqrt{6}} \mathbf{h}_k^{(j)}(1) \quad \mathbf{h}_k^{(j)}(2) \right]^T$ .

Then the average PEP has

$$\begin{aligned} & Pr(\mathbf{X}_k^* \rightarrow \hat{\mathbf{X}}_k^*) \\ & \leq \sum_{n=1}^N a_n \mathbb{E}_{\hat{\mathbf{H}}_k} \left[ \exp\left(-c_n \frac{3E_b}{4N_0} \sum_{l=1}^8 \sum_{i=1}^8 \lambda_k^i |\mathbf{h}_k^l \mathbf{v}_k^i|^2\right) \right] \\ & = \sum_{n=1}^N a_n \prod_{l=1}^8 \prod_{i=1}^8 \frac{1}{1 + c_n \frac{3E_b}{4N_0} \lambda_k^i b_k^{l,i}}. \end{aligned} \quad (24)$$

Hence the universal bound of BER should be weighted version of the PEP

$$\mathbf{BER} = \frac{1}{6} \frac{1}{2^{L \times N_t}} \sum_{i=1}^{2^{L \times N_t}} \sum_{j=1, j \neq i}^{2^{L \times N_t}} Pr(\mathbf{X}_k^i \rightarrow \mathbf{X}_k^j). \quad (25)$$

Denote  $r$  as the rank of  $(\mathbf{X}_k^i - \mathbf{X}_k^j)$ , the minimum  $r$  will provide the highest contribution to  $Pr(\mathbf{X}_k^i \rightarrow \mathbf{X}_k^j)$ , thus the diversity order is obtained by considering the virtue factor graph in Fig.(5) as

$$\text{div} = \min r = 4. \quad (26)$$

Note the diversity order in CIAMA is the same as STBC-SCMA's [29].

## V. SIMULATION

In this section, the performance of the proposed CIAMA is compared with traditional BIA and STBC-based SCMA. Also we consider a Alamouti scheme in a point-to-point  $2 \times 1$  MISO system as a benchmark in our simulation. Without loss of generality, we suppose all users have the same distance to the BS.

In the Fig.6, both CIAMA and STBC-SCMA utilize the two-stage ZF+MPA decoder. The BIA and the P2P Alamouti schemes use ZF decoder. We note that the STBC-SCMA has

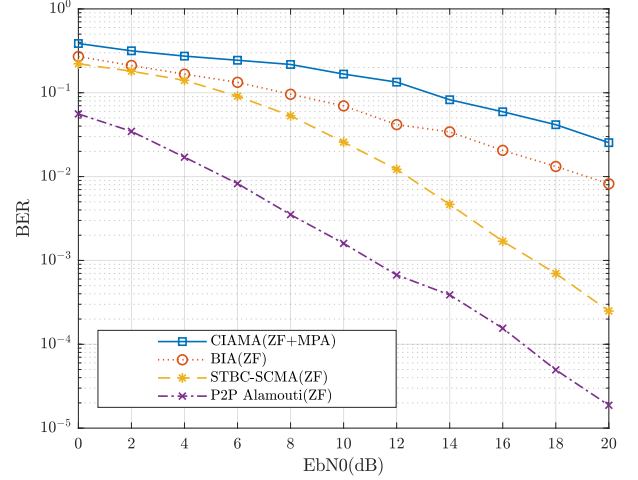


Fig. 6. BER Comparison (Zero-forcing+MPA)

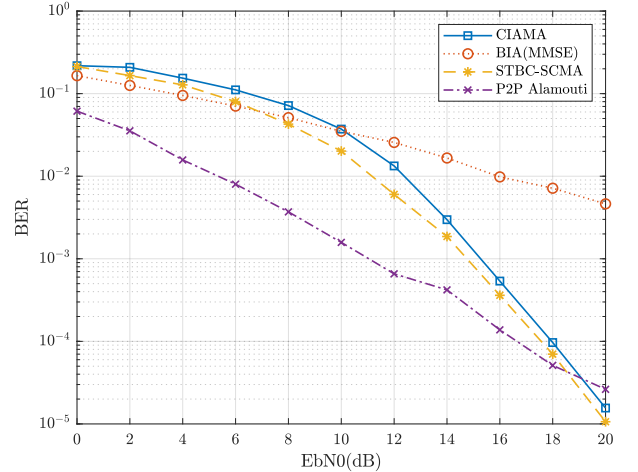


Fig. 7. BER Comparison (Joint MPA)

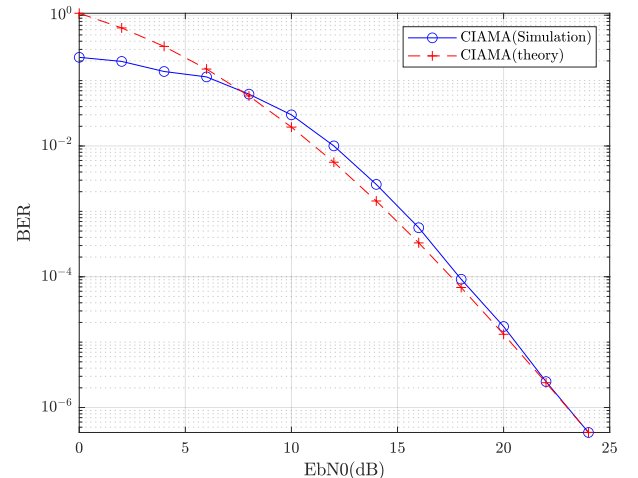


Fig. 8. BER comparison (Sim. vs Theory)

better performance than the BIA, because the SCMA can provide diversity over different tones. Although the ZF+MPA decoder has simple complexity, the CIAMA experience the worse BER than BIA. That's because the decoder doesn't consider the noise properly and the MPA part does not introduces channel state information. Also, the diversity order of CIAMA is the same as BIA's, because the MPA in two stage decoder provides no diversity gain. STBC-SCMA provides higher diversity than CIAMA and BIA, since STBC provides full diversity over multi antennas.

In the Fig.7, both CIAMA and STBC-SCMA utilize a joint MPA decoder and the BIA scheme using a MMSE decoder. From the figure we can find that the joint MPA can make full use of the benefits from the diversity. Note that STBC can provide spatial diversity, the BIA with joint MPA can also provide it while can not provide with ZF or MMSE. Also note that, the decoding complexity of the CIAMA with joint MPA is the same as STBC-SCMA with joint-MPA, but the CIAMA can provide more data flows, e.g., extra multiplexing gain.

Fig.8 presents the validation of the derived upper bound in expression (24). The approximation parameter sets are selected as  $N = 2$ ,  $a_1 = 1/12$ ,  $a_2 = 1/4$ ,  $c_1 = 1/2$ , and  $c_2 = 2/3$ . The proposed closed-form expression is verified to fit the simulation well; thus it provides a practical criterion to assess the performance of the proposed scheme.

## VI. CONCLUSION

This paper proposes a SparseCode-and-BIA-based multiple access (CIAMA) scheme to improve the system's performance. The introduction of BIA in this scheme provides both diversity and multiplexing gain, making it accommodating for systems with partial or no channel state information. Unlike existing MIMO-SCMA schemes, our scheme performs better data privacy. Two decoders are proposed for this scheme: a two-stage decoder and a joint message passing algorithm (MPA) decoder. The two-stage decoder has lower computational complexity, the joint MPA decoder provides better performance that is similar to the STBC-SCMA scheme.

## REFERENCES

- [1] M. Shafi et al., "5G: A tutorial overview of standards, trials, challenges, deployment, and practice," *IEEE J. Sel. Areas Commun.*, vol. 35, no. 6, pp. 1201-1221, 2017.
- [2] E. Hossain, M. Rasti, H. Tabassum, and A. Abdelnasser, "Evolution toward 5G multi-tier cellular wireless networks: An interference management perspective," *IEEE Wireless Commun.*, vol. 21, no. 3, pp. 118-127, 2014.
- [3] X. Ge, S. Tu, G. Mao, C.-X. Wang, and T. Han, "5G ultra-dense cellular networks," *IEEE Wireless Commun.*, vol. 23, no. 1, pp. 72-79, 2016.
- [4] X. You et al., "Towards 6G wireless communication networks: vision, enabling technologies, and new paradigm shifts," *Sci. China Inf. Sci.*, vol. 64, no. 110301, 2021.
- [5] N. Himayat, S. Talwar, A. Rao, and R. Soni, "Interference management for 4G cellular standards [WIMAX/LTE UPDATE]," *IEEE Commun. Mag.*, vol. 48, no. 8, pp. 86-92, 2010.
- [6] Z. Ding, X. Lei, G. K. Karagiannidis, R. Schober, J. Yuan, and V. K. Bhargava, "A Survey on Non-Orthogonal Multiple Access for 5G Networks: Research Challenges and Future Trends," *IEEE J. Sel. Areas Commun.*, vol. 35, no. 10, pp. 2181-2195, 2017
- [7] V. R. Cadambe and S. A. Jafar, "Interference alignment and degrees of freedom of the  $K$ -user interference channel," *IEEE Trans. Inf. Theory*, vol. 54, no. 8, pp. 3425-3441, 2008.
- [8] Z. Ding et al., "Application of non-orthogonal multiple access in LTE and 5G networks," *IEEE Commun. Mag.*, vol. 55, no. 2, pp. 185-191, 2017.
- [9] M. A. Maddah-Ali, A. S. Motahari, and A. K. Khandani, "Communication Over MIMO X Channels: Interference Alignment, Decomposition, and Performance Analysis," *IEEE Trans. Inf. Theory*, vol. 54, no. 8, pp. 3457-3470, 2008.
- [10] N. Zhao, F. R. Yu, H. Sun, and M. Li, "Adaptive power allocation schemes for spectrum sharing in interference-alignment-based cognitive radio networks," *IEEE Trans. Veh. Technol.*, vol. 65, no. 5, pp. 3700-3714, 2015.
- [11] C. Suh and D. Tse, "Interference Alignment for Cellular Networks," in 2008 46th Annual Allerton Conference on Communication, Control, and Computing, 23-26 Sept. 2008, pp. 1037-1044.
- [12] W. Shin, W. Noh, K. Jang, and H.-H. Choi, "Hierarchical interference alignment for downlink heterogeneous networks," *IEEE Trans. Wireless Commun.*, vol. 11, no. 12, pp. 4549-4559, 2012.
- [13] H. E. Elkotby, K. M. Elsayed, and M. H. Ismail, "Exploiting interference alignment for sum rate enhancement in D2D-enabled cellular networks," in 2012 IEEE Wireless Communications and Networking Conference (WCNC), 2012: IEEE, pp. 1624-1629.
- [14] L. Dai, B. Wang, Y. Yuan, S. Han, I. C, and Z. Wang, "Non-orthogonal multiple access for 5G: solutions, challenges, opportunities, and future research trends," *IEEE Commun. Mag.*, vol. 53, no. 9, pp. 74-81, 2015.
- [15] Z. Ding and H. V. Poor, "Design of massive-MIMO-NOMA with limited feedback," *IEEE Signal Process Lett.*, vol. 23, no. 5, pp. 629-633, 2016.
- [16] D. Zhang, Z. Zhou, C. Xu, Y. Zhang, J. Rodriguez, and T. Sato, "Capacity analysis of NOMA with mmWave massive MIMO systems," *IEEE J. Sel. Areas Commun.*, vol. 35, no. 7, pp. 1606-1618, 2017.
- [17] S. M. Razavi and T. Ratnarajah, "Performance analysis of interference alignment under CSI mismatch," *IEEE Trans. Veh. Technol.*, vol. 63, no. 9, pp. 4740-4748, 2014.
- [18] T. Gou, C. Wang and S. A. Jafar, "Aiming Perfectly in the Dark-Blind Interference Alignment Through Staggered Antenna Switching," *IEEE Trans. Signal Process.*, vol. 59, no. 6, pp. 2734-2744, 2011.
- [19] Q. F. Zhou, A. Huang, M. Peng, F. Qu and L. Fan, "On the Mode Switching of Reconfigurable-Antenna-Based Blind Interference Alignment," *IEEE Trans. Veh. Technol.*, vol. 66, no. 8, pp. 6958-6968, 2017.
- [20] J. Wu, X. Liu, C. Qu, C. -T. Cheng and Q. Zhou, "Balanced-Switching-Oriented Blind Interference-Alignment Scheme for 2-User MISO Interference Channel," *IEEE Commun. Lett.*, vol. 24, no. 10, pp. 2324-2328, 2020.
- [21] S. M. R. Islam, N. Avazov, O. A. Dobre, and K. Kwak, "Power-Domain Non-Orthogonal Multiple Access (NOMA) in 5G Systems: Potentials and Challenges," *IEEE Commun. Surv. Tutor.*, vol. 19, no. 2, pp. 721-742, 2017.
- [22] Z. Q. Al-Abbasi, D. K. C. So, and J. Tang, "Resource allocation for MU-MIMO non-orthogonal multiple access (NOMA) system with interference alignment," presented at the 2017 IEEE International Conference on Communications (ICC), 2017.
- [23] A. Nasser, O. Muta, M. Elsabrouty, and H. Gacanin, "Interference Mitigation and Power Allocation Scheme for Downlink MIMO-NOMA HetNet," *IEEE Trans. Veh. Technol.*, vol. 68, no. 7, pp. 6805-6816, 2019.
- [24] M. Morales-Céspedes, O. A. Dobre and A. García-Armada, "Semi-Blind Interference Aligned NOMA for Downlink MU-MISO Systems," *IEEE Transactions on Communications*, vol.68, no.3, pp.1852-1865, 2020.
- [25] Nikopour H, Baligh H. "Sparse code multiple access," 2013 IEEE 24th Annual International Symposium on Personal, Indoor, and Mobile Radio Communications (PIMRC). IEEE, 2013: 332-336.
- [26] M. Taherzadeh, H. Nikopour, A. Bayesteh and H. Baligh, "SCMA Codebook Design," 2014 IEEE 80th Vehicular Technology Conference (VTC2014-Fall), 2014, pp. 1-5
- [27] Moltafet M, Yamchi N M, Javan M R, et al. "Comparison study between PD-NOMA and SCMA," *IEEE Transactions on Vehicular Technology*, 2017, 67(2): 1830-1834.
- [28] Chen Y M, Chen J W. "On the design of near-optimal sparse code multiple access codebooks," *IEEE Transactions on Communications*, 2020, 68(5): 2950-2962.
- [29] Z. Pan, W. Liu, J. Lei, J. Luo, L. Wen and C. Tang, "Multi-Dimensional Space-Time Block Coding Aided Downlink MIMO-SCMA," *IEEE Transactions on Vehicular Technology*, vol.68, no.7, pp.6657-6669, 2019.
- [30] Y. -M. Chen, Y. -C. Hsu, M. -C. Wu, R. Singh and Y. -C. Chang, "On Near-Optimal Codebook and Receiver Designs for MIMO-SCMA Schemes," *IEEE Transactions on Wireless Communications*, vol.21, no.12, pp.10724-10738, 2022.
- [31] M. Chiani, D. Dardari and M. K. Simon, "New exponential bounds and approximations for the computation of error probability in fading

channels," IEEE Transactions on Wireless Communications, vol.2, no.4, pp.840-845, 2003.